Activity–Related Radial Velocity Variation in Cool Stars

Steven H. Saar[1]

(saar@cfa.harvard.edu)

and

Robert A. Donahue[1,2]

(donahue@cfa.harvard.edu)

Subject headings: convection — stars: activity — stars: late-type — stars: planetary systems — stars: spots — techniques: radial velocities

Received UNKNOWN; accepted UNKNOWN

Submitted to the *Astrophysical Journal.*

[1]Harvard-Smithsonian Center for Astrophysics, 60 Garden St., Cambridge, MA 02138 USA.

[2]Mount Wilson Institute, 740 Holladay Road, Pasadena, CA 91106, USA.

ABSTRACT

Planets have been detected orbiting several solar-type stars using high-precision radial velocity (v_r) measurements. While changes in v_r can be measured with an accuracy of a few m s^{-1}, there has been relatively little study of how other astrophysical processes, such as magnetic activity, may effect the observed velocities. In this paper, we use published data and simple models to explore the contributions to v_r from two activity-related sources, starspots and convective inhomogeneities, as these features rotate across the disk and evolve in time.

Radial velocity perturbations due to both of these sources increase with rotation and the level of surface activity. Our models indicate that for solar-age G stars, the amplitude of perturbations due to spots is $A_S \lesssim 5$ m s^{-1}, increasing to $A_S \sim 30$ to 50 m s^{-1} for Hyades-age G stars. If f_S is the starspot area coverage, we find $A_S \propto {f_S}^{0.9} v \sin i$. The effects of convective inhomogeneities (as observed in line bisector variations) appear to depend on both rotation and spectral type. Young (active) F and G dwarfs can have convective v_r perturbations with amplitudes $A_C \gtrsim 50$ m s^{-1}, while v_r amplitudes are reduced for stars with lower $v \sin i$ and cooler $T_{\rm eff}$. We show that v_r data from the literature display similar trends with $v \sin i$ and $T_{\rm eff}$. A_S and A_C will be strongest at or near timescales related to magnetic activity variations: rotation, active region growth and decay, and activity cycles. Thus, knowledge of these timescales and typical A_S and A_C values are important in searching for extra-solar planets, especially those around younger, more active stars or those with small v_r reflex amplitudes (i.e., $\lesssim 20$ m s^{-1}). We discuss implications of our results for current planet detections and planet search strategies.

1. Introduction

Planets have been recently detected orbiting several solar-type stars using high-precision measurements of radial velocity, v_r (Mayor & Queloz 1995; Marcy & Butler 1996; Butler & Marcy 1996; Butler et al. 1996). Planets with large v_r amplitudes (> 100 m s^{-1}) and short periods ($P_{orb} \lesssim 1$ yr) are easiest to detect by such methods, and several of the recently discovered low-mass companions are in this category (e.g., 70 Vir B). Most of the stellar primaries have an interesting feature in common, however: they are essentially non-variable and chromospherically inactive (Henry et al. 1997). This fact suggests that a secondary selection effect may exist: a lack of significant magnetic activity improves the probability of detecting low amplitude v_r variations.

There is observational support for this hypothesis. First, rotation of starspots across the stellar disk clearly affects the line profiles of many active stars (e.g., Vogt, Penrod, & Hatzes 1987), and these perturbations in turn affect line centroids. On rapid rotators, the signatures of starspots can be identified when Doppler–resolved. On stars with lower $v \sin i$, however, they merely induce a subtle unresolved asymmetry, and hence a line centroid shift of *uncertain* origin. Second, line bisectors vary on the Sun (Livingston 1991) and especially on more active stars (e.g., Toner & Gray 1988; Gray et al. 1996a). These fluctuations are thought to be primarily the result of changes in the mean convective pattern, brought on by temporal and spatial evolution of the stellar magnetic regions where the convection is altered (Livingston 1982; Dravins 1985; Toner & LaBonte 1990). While the exact relationship between line bisectors and v_r is uncertain (e.g., Butler et al. 1996), fluctuating line asymmetries will almost certainly have some affect on v_r. Solar IR line positions appear vary by $\approx$30 m s^{-1} over the solar cycle, correlated with changes in magnetic flux (Deming & Plymate 1994), and in mean bisector shape (Deming et al. 1987). (However, see McMillan et al. 1993, for a differing result.)

Since radial velocity instruments and techniques are now capable of measuring v_r with accuracies of ~ 3 m s^{-1} (Butler et al. 1996), it is timely to explore possible intrinsic sources of stellar radial velocity variability. Hatzes (1996) has studied the effects of non-radial pulsations on line bisectors and v_r. In this paper we explore the effects of stellar surface features, specifically

starspots and convective inhomogeneities, on precision radial velocity measurements of cool stars, and their implications for planetary searches.

2. Analysis

2.1. The Effect of Rotation in Spotted Stars

One source of perturbations affecting $v_{\rm r}$ measurements arises due to dark spots on a star with $v \sin i \neq 0$. Any non-axisymmetric inhomogeneity in the spot distribution, or its temporal evolution, will generate a time-variable photometric and spectroscopic signature. The magnitude of photometric variation, and thus the surface area covered by the inhomogeneity, $f_{\rm S}$, ranges from near zero for old, inactive stars (e.g., the Sun, with $f_{\rm S} \approx 0.15\%$; Dorren & Guinan 1994a) to several percent for active stars (e.g., the young G0V HD 129333 with $f_{\rm S} \approx 6\%$; Dorren & Guinan 1994b). Note that $f_{\rm S}$ is different from the *total* area covered by spots; it refers instead to the non-uniform portion of the spot distribution responsible for the observed variability. The two can differ significantly for active stars (e.g., O'Neal, Saar, & Neff 1996).

To explore the velocity perturbations caused by spots, we have constructed models of a solar-like star ($T_{\rm eff}$ = 5750 K) with a single (square) spot with $f_{\rm S}$ between 0 and 2%. Since we are interested in the *maximum* $v_{\rm r}$ effect spots can have, we set the spot temperature $T_{\rm S} = 0$ and placed the spot on the equator (near-equatorial spots are seen on both the Sun and active stars; Allen 1976, Strassmeier 1996). We computed medium-strength Fe I lines (W_λ = 180 mÅ) at 6000Å in a Milne-Eddington atmosphere with micro- and radial-tangential macroturbulent velocities of $v_{\rm mic}$ = 1 km s^{-1} and $v_{\rm mac}$ = 3 km s^{-1}, respectively. Intensity profiles were computed at 15 limb angles defining the centers of 15 radial sectors of equal projected area (Bruning 1984) with a limb-darkening coefficient $\epsilon = 0.6$. The lines were next integrated over the stellar disk on a 1×1 degree grid for $0 \leq v \sin i \leq 10$ km s^{-1} ($i = 90°$), keeping the line profile constant within each radial sector, but applying velocity shifts appropriate to each grid point.

To measure the velocity perturbation, $\Delta v_{\rm r}$, we fit each resulting integrated flux profile

with a Gaussian to measure the apparent shift in the line center as a function of rotational phase, ϕ (Fig. 1). This fitting procedure was chosen to mimic the "full spectrum modeling" method used by Butler et al. (1996) to achieve the most accurate $v_{\rm r}$ measurements. For the equatorial, $T_{\rm S} = 0$ spots considered here, we find that the (semi-)amplitude of the $v_{\rm r}$ variations, $A_{\rm S} = [\Delta v_{\rm r,max}(\phi) - \Delta v_{\rm r,min}(\phi)]/2$, can be approximated by

$$A_{\rm S} \approx 6.5 {f_{\rm S}}^{0.9}\ v \sin i, \tag{1}$$

where $f_{\rm S}$ is in percent, $v \sin i$ in km s^{-1} and $A_{\rm S}$ in m s^{-1}. This relation is accurate to $\pm$ 1 m s^{-1} for $A_{\rm S} < 5$ m s^{-1}, and to better than 20% for 5 m s^{-1} $\leq A_{\rm S} \leq$ 85 m s^{-1}. $A_{\rm S}$ repesents the amplitude of the largest $v_{\rm r}$ perturbation expected for a given (equatorial) $f_{\rm S}$ and $v \sin i$ on a solar-like star. Contours of $A_{\rm S}$ are plotted in Fig. 2 as a function of $f_{\rm S}$ and $v \sin i$.

In Fig. 2 we also plot the $v \sin i$ and $f_{\rm S}$ values for selected G dwarfs, including several where low–mass companions have been discovered. We estimated $f_{\rm S}$ from the photometric amplitude by again assuming the limiting case of completely black, equatorial spots (which gives a *lower* limit to the true $f_{\rm S}$). For latitude $\theta = 0$ and our choice of ϵ, this implies that $f_{\rm S} \approx 0.40 \Delta V$. The photometric amplitudes (usually ΔV or, in the case of HD 152391, ΔF_{6585}, and for σ Dra and ξ Boo A, Strömgren Δy), $v \sin i$ values and their sources are given in the Table 1, as are our model estimates of $A_{\rm S}$. For non-equatorial spots, $f_{\rm S}$ must increase by a factor of $\approx (\cos\theta)^{-1}$ to yield the same ΔV. Since non-equatorial spots also have a reduced maximum $\Delta v_{\rm r}$ (by a factor of $\approx \cos\theta$), *an observed ΔV implies a fixed $A_{\rm S}$ value nearly independent, to first order, of the spot latitude* for a given star (this of course breaks down near $\theta = 90°$).

Other methods of $v_{\rm r}$ determination using information across the full line profile yields similar results. Using a line-depth weighted centroid, for example, gave almost identical $\Delta v_{\rm r}(\phi)$ and $A_{\rm S}$ values to the Gaussian fits. A method which determined $v_{\rm r}$ largely from the line core (using a cubic spline to interpolate the "true" minimum) yielded rather different results, however (Fig. 1). In this case, $\Delta v_{\rm r}(\phi)$ peaked closer to disk center and the resulting $A_{\rm S}$ values were typically (and sometimes significantly) larger and more strongly dependent on $v \sin i$. This is probably due to the line core method's greater sensitivity to the presence of the spot near disk center, unlike the

Gaussian fit method, where the the v_r measurement contains contributions by parts of the line profile unaffected by the spot.

Since both $v \sin i$ and f_S decrease with stellar age, we expect a rapid decrease in A_S as a star ages. The Pleiades age dwarf HD 129333, with $\Delta V \approx 0.06$ and $v \sin i \approx 15 - 17$ km s^{-1} (Güdel et al. 1995), could have a $A_S > 200$ m s^{-1} (extrapolating from eqn. 1). A Hyades age star (e.g., VB 64 or 9 Ceti, age ≈ 0.8 Gyr) can have $A_S \approx 30$ to 50 m s^{-1} or more. If β Comae, with a $v \sin i$ of 4 km s^{-1} (Gray 1984; Soderblom 1983) and $\Delta V \approx 1\%$ (Dorren & Guinan 1994a) is typical of solar-like stars ~ 2 Gyr old (Donahue 1993), then for equatorial spots $f_S \sim 0.4\%$ and $A_S \approx 10$ m s^{-1}. The Sun (and similar older stars with minimal f_S) should show $A_S \ll 10$ m s^{-1} ($A_{S,\odot} < 1$ m s^{-1}).

2.2. The Effect of Inhomogeneous Convection

Another potentially significant contributor to velocity perturbations in cool stars arises due to spatial variations in convection. These variations are likely due to the rotation and evolution of the areas with altered granulation associated with magnetic regions (e.g., Livingston 1982). On the Sun, for example, granulation is suppressed and changes are seen in both line core convective blueshift and in line bisector shape as the magnetic area increases (Brandt & Solanki 1990). On active stars, flows in active regions may be enhanced (Toner & LaBonte 1990). Rotation of an inhomogeneous, non-axisymmetric velocity field across the stellar disk will produce a variable line asymmetry and an apparently variable v_r (e.g., Gray 1988). However, the correlation between convective variability and magnetic activity is *not* as straightforward as has been previously suggested (Dravins 1985; Campbell, Walker, & Yang 1988). Since bisector spans are enhanced by the "rotation effect" (Gray 1986), an active region (AR) near the pole will have a much smaller effect on line bisectors than an equatorial AR of equal size. Also, completely inactive stars, and those completely covered by ARs, will both show *no* bisector variation. Thus, the positions of the AR, the relative inhomogeneity, and the $v \sin i$ of the star – and not just its mean activity level – are all factors that affect bisector variability and the related changes in v_r.

Since realistic modeling of stellar convection and line bisectors is not a trivial undertaking (Nordlund & Dravins 1990; Dravins & Nordlund 1990a), we turn to measurements of the line bisector span, $v_{\rm span}$ to help estimate $\Delta v_{\rm r}$ due to variable convection. The $v_{\rm span}$ value is typically defined as the displacement in velocity along a bisector from 0.5 to 0.8 of the continuum flux (K stars) or 0.55 to 0.85 (G stars; Gray et al. 1992). We assume that the mean line centroid displacement (the perturbation to $v_{\rm r}$), is $\Delta v_{\rm r} = v_{\rm span}/2$, and use this to compute the amplitude of $\Delta v_{\rm r}$ variations. This is equivalent to assuming that $\Delta v_{\rm r}$ is given by the half the difference between velocities determined in the line core and a point near its wings. Although admittedly an arbitrary definition, this seems to be a reasonable estimate in the absence of any established empirical or theoretical relationship between $\Delta v_{\rm r}$ and $v_{\rm span}$ (we explore this further in §2.3).

Unfortunately, information on bisector variability is limited. We have focused on two estimates of the size of bisector variations: changes on the timescale of rotation, and the maximum observed range of $v_{\rm r}$ from bisector measurements (on any timescale). In the case of rotation, we define the semi-amplitude of $v_{\rm r}$ variation due to non-uniform convection as $A_{\rm C,rot} \equiv (\Delta v_{\rm r,max} - \Delta v_{\rm r,min})/2 = (v_{\rm span,max} - v_{\rm span,min})/4 = \Delta v_{\rm span}/4$, where the maximum and minimum $\Delta v_{\rm r}$ values are separated by no more than a single rotation of the star. Values of $v_{\rm span}$ used to compute $A_{\rm C,rot}$ were either taken directly from the literature, measured from a plot (the Sun; Livingston 1991), or estimated as the maximum intra-seasonal rms of tabulated $v_{\rm span}$ data (ϵ Eri; Gray & Baliunas 1995). We also calculate the maximum amplitude, $A_{\rm C,max}$, allowing $v_{\rm span,max}$ and $v_{\rm span,min}$ to be separated by any time period. $A_{\rm C,max}$ was either computed from the available data, or measured from plots (χ^1 Ori, β Comae, Sun, σ Dra). In the case of χ^1 Ori, however, we were careful to use data taken only within a timespan of a few days to avoid complications due to its binary orbital motion (Irwin et al. 1992); hence, for this star $A_{\rm C,max} = A_{\rm C,rot}$. For ξ Boo A, $A_{\rm C,max}$ includes the sum of the long-term (Gray et al. 1996a) and short-term (Toner & Gray 1988) modulation amplitudes. In the case of 51 Peg, we take $A_{\rm C,max} = A_{\rm C,rot}$ equal to one half of the $v_{\rm span}$ amplitude upper limit given by Hatzes, Cochran & Johns–Krull (1997).

We plot $A_{\rm C}$ versus $B-V$ color, $v \sin i$, and normalized Ca II flux, $R'_{\rm HK}$, in Figure 3. $R'_{\rm HK}$

was computed using the calibration of Noyes et al. (1984) and the most recent available $\langle S \rangle$ measurements. G stars generally have larger $A_{\rm C}$ than K stars even when they are equally active (cf. χ^1 Ori and ϵ Eri). This is expected: $\Delta v_{\rm r}$ should decrease with decreasing $T_{\rm eff}$ echoing the decline in bisector spans (Gray 1982; 1988), and $v_{\rm mac}$ (Gray 1984; Saar & Osten 1997). The rotational enhancement of bisectors (Gray 1986) should increase $A_{\rm C}$ in stars with higher $v \sin i$. This effect accounts for much of the spread in $A_{\rm C}$ at a given $T_{\rm eff}$: compare χ^1 Ori ($v \sin i = 9.4$ km s^{-1}) with β Comae ($v \sin i \approx 4.0$ km s^{-1}). The enhancement may saturate above some velocity, however (Bruning & Saar 1990). Finally, an increased number of ARs (larger $R'_{\rm HK}$) on the surface generally results in larger $\Delta v_{\rm r}$; active G stars such as β Comae, ξ Boo A, and χ^1 Ori have larger $A_{\rm C}$ than either the Sun or τ Ceti. Rotation and $T_{\rm eff}$ seem to be more physically significant parameters: χ^1 Ori, ξ Boo A, and ϵ Eri all have similar $R'_{\rm HK}$, but have quite different $A_{\rm C}$ values.

2.3. The Effect of Starspots on Line Bisectors and $A_{\rm C}$

The presence of spots on a rotating star will also have an effect on line bisectors, and thus on measurements of $v_{\rm span}$ and $A_{\rm C}$. $A_{\rm C}$ is therefore not a "pure" measurement of variations due to a star's convective properties; spots clearly alter bisector shapes at some level as well (e.g., Dempsey et al. 1992). To explore this effect, we have computed $v_{\rm span}$ values from our spot models in §2.1 following the prescription of Gray et al. (1992) for G stars. It is immediately apparent that the dependence of $v_{\rm span}$ on spot rotational phase ϕ is quite different than for the $\Delta v_{\rm r}(\phi)$ derived from Gaussian fits in §2.1 (Fig. 1). Similar to the $\Delta v_{\rm r}(\phi)$ derived from line core shift estimates, $v_{\rm span}(\phi)$ peaks closer to disk center. To a good approximation, we find that the (semi-)amplitude of the bisector velocity span variation due to spots, $A_{\rm S,span} = (v_{\rm span,max} - v_{\rm span,min})/2$, is given by

$$A_{\rm S,span} \sim 0.11 {f_{\rm S}}^{0.9} \, (v \sin i)^{3.3} \tag{2}$$

in m s^{-1}, with the quantities defined as in (1). Note that $A_{\rm S,span}$ has a much stronger dependence on rotation than $A_{\rm S}$: $A_{\rm S,span} \propto A_{\rm S} (v \sin i)^{2.3}$.

A comparison of stars common in Tables 1 and 2 suggests that typically $A_{\rm C} \geq A_{\rm S}$ in G stars

(although this changes for K stars; see §4.1). Since $A_S \geq A_{S,span}/2$ over most of the parameter regime we have studied ($v \sin i \leq 8$ km s^{-1}), we may (to a first approximation) neglect the effect of spots on A_C values for slow and moderately rotating G stars.

This analysis may also contain some insight regarding the relationship between v_{span} and v_r. Although $A_{S,span}$ does not include the effects of velocity fields *correlated* with an inhomogeneous temperature distribution, it does contain at least some of the physics of a convective model. To the limited extent that this is true, the inequality $A_S \geq A_{S,span}/2$ for G stars with $v \sin i \leq 8$ km s^{-1} hints that for these stars, our assumption $A_C \approx \Delta v_{span}/4$ in the case of inhomogeneous convection may be reasonable (and may even *underestimate* A_C).

2.4. An Observational Test

To test our predictions on the effect of spots and inhomogeneous convection on stellar v_r, we study the high-precision v_r measurements of Campbell et al. (1988) and Walker et al. (1995). Although sometimes cited as evidence that intrinsic stellar variations affect v_r at only the 10 m s^{-1} level or less (e.g., Butler et al. 1996), detailed study of this data set yields a more complex picture. Our analysis differs from these studies in that Campbell et al. and Walker et al. remove linear or quadratic trends, and in some cases consider them to be possibly planetary in origin. Instead, we assume that trends observed are *not* due to planets, but instead are due to temporal changes in starspot distribution and/or convective properties. We then study correlations between observed v_r amplitudes and $B-V$ (i.e., T_{eff}), $v \sin i$, and activity to see if they are consistent with this hypothesis. Unfortunately, the data set is somewhat limited for our purposes: most of the dwarfs included in it are either inactive, have low $v \sin i$, or are in binary systems needing significant corrections for orbital motion (thereby adding another source of v_r noise). The only star with $v \sin i > 4$ km s^{-1} (χ^1 Ori) has a significant (> 1 km s^{-1}) v_r perturbation due to a stellar companion (Irwin et al. 1992). For this and other reasons detailed below, we believe the χ^1 Ori v_r data may not be very reliable for our purposes.

Despite these problems, the data still show trends consistent with our predictions. Walker et al. (1995) find a trend between chromospheric emission and $v_{\rm r}$ for κ^1 Cet, and significant secular trends for several other stars (36 UMa, β Vir, β Com, ξ Boo A, 36 Oph B). All of these stars are either active, or are F stars with intrinsically larger $\langle v_{\rm span} \rangle$ (Gray 1982, 1988). The possible 9.88 year periodicity for ϵ Eri (Walker et al. 1995) is about twice the tentative five year magnetic cycle suggested by Gray & Baliunas (1995).

A more detailed analysis of the Walker et al. (1995) data set shows further agreement. First, we removed all points where the internal errors (the dispersion in $v_{\rm r}$ among the individual spectral lines) have $\sigma_i \geq 2\langle \sigma_i \rangle$. We also removed points deviating by more than 3σ from a five point running average trend line, to remove extreme outliers. (Similar results are obtained without this step.) We then computed weighted (by σ_i) RMS velocity dispersions, $\sigma'_{v_{\rm r}}$, and maximum velocity amplitudes, $A'_{\rm max} = (v_{\rm r,max} - v_{\rm r,min})/2$. No trends were removed other than those due to known binary motion. Specifically, ξ Boo A and 61 Cyg A were corrected following Campbell et al. (1988), 36 Oph A and B, and 61 Cyg B were corrected following Walker et al. (1995), and for χ^1 Ori we used Irwin et al. (1992). We plot the results in Figure 4 against $B-V$, $v \sin i$, and $R'_{\rm HK}$ (analogous to Fig. 3). The $A'_{\rm max}$ and $\sigma'_{v_{\rm r}}$ values are also listed in Table 2.

The upper envelope of $A'_{\rm max}$ and $\sigma'_{v_{\rm r}}$ values appears to decrease with increasing $B-V$ (decreasing $T_{\rm eff}$; Fig. 4, right). This is expected from the bisector variation results (Fig. 3) – if stars have similar fractional $\Delta v_{\rm span}$, the intrinsically larger $\langle v_{\rm span} \rangle$ of F and G stars would naturally lead to larger $A'_{\rm max}$ and $\sigma'_{v_{\rm r}}$. The spread at a given $B-V$ is then due to the range in $v \sin i$ and activity at fixed $T_{\rm eff}$. This idea is supported by the increase in $A'_{\rm max}$ and $\sigma'_{v_{\rm r}}$ values with $v \sin i$ (Fig. 4, center), since a larger projected rotation rate increases both $A_{\rm S}$ (§2.1), and $A_{\rm C}$ via the "rotational enhancement" effect (Gray 1986). Finally, stars with larger $R'_{\rm HK}$ have somewhat enhanced $A'_{\rm max}$ and $\sigma'_{v_{\rm r}}$ on average (Fig. 4, right), consistent with the expected rise in $\Delta v_{\rm r}$ due to both spots and convection with activity (e.g., Dravins 1985), but masked somewhat by $T_{\rm eff}$ and rotational effects. Thus, trends with both $B-V$, $v \sin i$, and the weak trend with activity (Fig. 4) confirm our general predictions (Figs. 2 and 3). In general, these relationships are clearer

in the single stars (which do not suffer from the additional uncertainty created by binary motion corrections).

If we define a "total" combined (spot + convection) maximum $v_{\rm r}$ amplitude $A_{\rm tot} = \sqrt{(A_{\rm S})^2 + (A_{\rm C,max})^2}$, we find that (excluding χ^1 Ori), $A'_{\rm max} \approx A_{\rm tot}$ for the five stars with values available for all three parameters (Fig. 5). Here, we have taken $\Delta V \approx 0.014$ for ϵ Eri (Gray & Baliunas 1995), and $\Delta(b+y) \approx 0.005$ for σ Dra (Gray et al. 1992). The rms about the relation $A_{\rm tot} = A'_{\rm max}$ (excluding χ^1 Ori) is $\sigma = 13.8$ m s^{-1}, consistent with the mean measurement rms quoted by Walker et al. (1995) of ≈ 13 m s^{-1}. It would be interesting to construct an analogous combined (spot + convection) rms $\sigma_{\rm tot} = \sqrt{(\sigma_{\rm S})^2 + (\sigma_{v_{\rm span}})^2}$ to compare with the observed $\sigma'_{v_{\rm r}}$ (Table 2). Unfortunately, stars with published data on both ΔV and $v_{\rm span}$ usable to compute $\sigma_{\rm tot}$ are scarce. Using our spot model instead, the rms variation of $\Delta v_{\rm r}$ for spots is $\sigma_{\rm S} \approx 0.7 A_{\rm S}$. We have studied the two cases with available bisector data (Gray & Baliunas 1994, 1995), using the model $\sigma_{\rm S}$ for ϵ Eri and assuming $\sigma_{\rm S} = 0$ for τ Ceti. We find $\sigma_{\rm tot} = 10.5$ m s^{-1} for ϵ Eri and $\sigma_{\rm tot} = 7.6$ m s^{-1} for τ Ceti, in reasonable agreement with the measured $\sigma'_{v_{\rm r}}$ values.

The apparent $A'_{\rm max}$ value of χ^1 Ori (~ 50 m s^{-1}) is considerably smaller than predictions of either $A_{\rm S}$ (≈ 84 m s^{-1}) or $A_{\rm C}$ (≈ 100 m s^{-1}) alone. There are several reasons, however, for concern about the values of $A'_{\rm max}$, $A_{\rm S}$, and $A_{\rm C}$ for this star. First, the binary solution for χ^1 Ori may include some $\Delta v_{\rm r}$ due to spots and non-uniform convection, reducing the measured $A'_{\rm max}$ and $\sigma'_{v_{\rm r}}$. Our simple assumption that $A_{\rm C} \sim \Delta v_{\rm span}/4$ may overestimate $A_{\rm C}$ due to the increased contributions of spots to $v_{\rm span}$ on this rapid rotator (§2.3). Also, depending on the sign of $v_{\rm span}$ due to convection and how it changes with activity, $A_{\rm C}$ and $A_{\rm S}$ may actually cancel each other to some extent. Our definition of $A_{\rm tot}$ as a quadratic sum may then be too simplistic, not taking into account correlations between spots and convection or the sign of their perturbations. $A_{\rm S}$ may also be reduced if spots on χ^1 Ori are concentrated at high latitudes (e.g., Schüssler & Solanki 1992). Models of a rapidly rotating Sun suggest fluxtube emergence on a G2 star with $P_{\rm rot}$ similar to χ^1 Ori (≈ 5.4 days; Donahue, Saar, & Baliunas 1996) should be restricted to $\theta \gtrsim 30°$ (DeLuca, Fan, & Saar 1997). Finally, the available bisector data is quite limited, and noisier than normal due to

the more rotationally broadened profiles of χ^1 Ori, producing considerable uncertainty over the true magnitude of $A_{\rm C}$. For these reasons, we have dropped χ^1 Ori from our comparison analysis. We note, however, that if we make rough corrections for some of these effects – subtracting from $A_{\rm C}$ a $A_{\rm S,span}/2$ value based on (2) to avoid "double counting" the effects of spots, and scaling $A_{\rm S}$ by $\cos(30^\circ)$ to reflect the restricted emergence latitude – the resulting modified $A_{\rm tot}$ for χ^1 Ori is ≈ 73 m s^{-1}, in better agreement with $A'_{\rm max}$ (Fig. 5).

3. Discussion

3.1. Relationship of $\Delta v_{\rm r}$ to Other Stellar Properties and Timescales

We can attempt to estimate how $\Delta v_{\rm r}$ due to spots and inhomogeneous convection evolves with time t and other stellar parameters. Since to first order $v \sin i \propto t^{-0.5}$ (Skumanich 1972) and $f_{\rm S} \sim \Delta V \propto \log(1/P_{\rm rot})$ (Dorren & Guinan 1994a), it follows that $A_{\rm S} \propto t^{-0.5} F(\log t)$, where $F(\log t)$ is some function of $\log t$. Scaling relations for $A_{\rm C}$ are more uncertain. It is reasonably clear that $\langle v_{\rm span} \rangle \propto \langle v_{\rm mac} \rangle$ (Gray 1988), and $\langle v_{\rm mac} \rangle$ decreases with increasing $B-V$ (Gray 1984; Saar & Osten 1997). There is also some evidence that $\langle v_{\rm mac} \rangle$ increases with activity (Gray 1984; Saar & Osten 1997), suggesting that $v_{\rm span}$ may as well, although the exact relationship between them is uncertain. The scaling between $v_{\rm span}$ and $v \sin i$ is also unclear; $v_{\rm span} \propto v \sin i$ (Gray 1988; Saar & Bruning 1990), a linear relationship saturating at ≈ 7.5 km s^{-1} (Bruning & Saar 1990), and $v_{\rm span} \propto (v \sin i)^2$ (Smith et al. 1987) have all been proposed.

Measurements of ΔV among young cluster stars suggest that for stars of the same age, active K dwarfs can have 2 to 4 times larger $f_{\rm S}$ than G dwarfs, while F dwarfs have smaller $f_{\rm S}$ (O'Dell et al. 1995; see their Fig. 3). K stars also predominate among objects with the large ΔV values (Strassmeier et al. 1993), and among rapid rotators, $\langle \Delta V \rangle_{\rm K} > \langle \Delta V \rangle_{\rm G}$ (O'Dell et al. 1995, their Figs. 1 and 2). Published data on the photometric variability of older K dwarfs is scarce, but the limited evidence available suggests ΔV may be enhanced relative to G dwarfs among them as well. For example, 12 Oph (Dorren & Guinan 1982) and κ^1 Cet (Dorren & Guinan 1994a) have similar

photometric amplitudes ($\approx 2\%$), but the inverse Rossby number of κ^1 Cet is almost 50% larger, implying it is younger (Donahue 1993). Thus, for stars of fixed age, A_S appears to be typically larger in K dwarfs, and smaller for F dwarfs. Possible physical reasons for the difference include the ability to generate larger inhomogeneities in K stars (Ruciński & VandenBerg 1986), and the greater difficulty to form spots in F stars (Bünte & Saar 1993).

Combining these trends with the A_S and A_C values of Figs. 2 and 3 suggests that inhomogeneous convection likely dominates the total activity-related v_r variation in F and most G stars (excepting possibly the most spotted, rapidly rotating ones). Consistent with this idea, Butler et al. (1997) report sporadic v_r excursions in the range of 80 to 100 m s^{-1} in four photometrically non-variable F stars. G. Marcy (1997, private communication) adds that nearly all F stars in their sample show similar sporadic v_r excursions. In contrast, convective asymmetries are reduced in K stars, while f_S increases, and so A_{tot} will likely be dominated by the component due to spots.

Because the velocity perturbations are linked to stellar activity, Δv_r due to spots and convection will be stronger near the corresponding activity time scales, such as rotation (P_{rot}), AR growth and decay, and magnetic cycles (P_{cyc}). Planets with orbital periods different from these dominant stellar periods may permit easier planet detection, even for active stars and low v_r amplitudes. Unfortunately, these periods are not always well defined. Mean rotational periods will vary due to the differential rotation of the activity tracers used, and changes in the mean AR location over the stellar cycle (Donahue 1993; Donahue et al. 1996). The lengths of individual sunspot cycles are known to vary between 7 and 15 years (Eddy 1977; Donahue & Baliunas 1992), and it is likely that such a spread in cycle length is present in other stars as well. In addition, some stars show multiple cycle periods (Baliunas et al. 1995). Since AR growth/decay timescales are poorly known (and can be ill-defined even when known; see Dobson et al. 1990, Donahue, Dobson, & Baliunas 1997), it is advisable to treat low amplitude v_r modulation on timescales between P_{rot} and P_{cyc} for active stars with some caution. Similarly, v_r variations at or near P_{rot} and P_{cyc} are suspect for stars somewhat more active than the Sun. Knowledge of these periods

and amplitudes would be valuable in searching for any low-level planetary velocity modulation.

3.2. Implication for Current Planetary Detections

It is important to note that our results *do not* cast doubt on the reality of the current crop of planetary companions (Mayor & Queloz 1995; Marcy & Butler 1996; Butler & Marcy 1996). All of the stellar primaries in these cases have negligible photometric variability (Table 1) and hence small $A_{\rm S}$ values (Fig. 2), and if they are similar to 51 Peg (Hatzes et al. 1997), they also have $A_{\rm C,max} \lesssim 20$ m s^{-1}. This implies $A_{\rm tot} \lesssim 20$ m s^{-1} as well, significantly less than the observed $v_{\rm r}$ amplitudes due to planetary companions.

Our results *do*, however, possibly explain some anomalies among current planet detections. The F7 dwarf τ Boo appears to have a companion of $\sim$4 Jupiter masses in an orbit with a semi-amplitude velocity of $K = 469$ m s^{-1} and $P_{\rm orb} = 3.31$ days (Butler et al. 1997), similar to the estimated rotational period of $P_{\rm rot} \sim 3.5$ days (e.g., Baliunas et al. 1997). Since the star has $v \sin i = 14.8$ km s^{-1} (Gray 1982), we predict that $A_{\rm C}$ could be large (though $A_{\rm S} \approx 0$, since $\Delta V < 0.002$; Baliunas et al. 1997). Assuming a linear relation between $A_{\rm C}$ and $v \sin i$, we can extrapolate $A_{\rm C} \sim 150$ m s^{-1} from Fig. 3. This is consistent with the unexplained fluctuations with $\sigma'_{v_{\rm r}} \sim 80$ m s^{-1} seen in the velocity residuals in some time intervals (Butler et al. 1997). Similarly, we estimate $A_{\rm C} \sim 90$ m s^{-1} for υ And ($v \sin i = 9.2$ km s^{-1}; Soderblom 1983), which shows variations in its mean $v_{\rm r}$ of ~ 50 m s^{-1} on a 2 year timescale (Butler et al. 1997). Thus, velocity residuals for both τ Boo and υ And may be explained by the occasional presence of regions with altered convective properties. On the other hand, the long term trend in the $v_{\rm r}$ residuals for ρ^1 Cnc (Butler et al. 1997) cannot be explained by magnetic activity. In fact, ΔV and $v \sin i$ are both too small (Baliunas et al. 1997) to yield a significant value for either $A_{\rm S}$ or $A_{\rm C}$.

3.3. Uncertainties in the Analysis

There are several uncertainties in our analysis. Some have already been mentioned in our discussion of χ^1 Ori (§2.4). First, non-uniform convection may cause bisectors to vary such that the $\Delta v_{\rm r} \neq v_{\rm span}/2$. Simultaneous measurement of $v_{\rm span}$ and high-accuracy $v_{\rm r}$ could help resolve this question, but unfortunately, the gas absorption cell methods used for accurate $v_{\rm r}$ measurements (e.g., Walker et al. 1995; Butler et al. 1996) degrade $v_{\rm span}$ determinations because of the numerous line blends they impose on the spectra. Therefore, in the absence of appropriate data, our assumption seems as reasonable as any for estimating $A_{\rm C}$, especially since $v_{\rm span}$ fluctuations due to spots have $\Delta v_{\rm r} \leq v_{\rm span}/2$ for $v \sin i \leq 8$ km s^{-1} (§2.3). The relationship between $v_{\rm span}$, $f_{\rm S}$ and $\Delta v_{\rm r}$ is likely a complex function of $T_{\rm eff}$, $v \sin i$, and activity. For example, since AR show locally reduced $v_{\rm span}$ on the Sun, spots associated with the same AR could conceivably enhance *or* reduce the total $\Delta v_{\rm r}$ depending on the interplay of light and velocity variations. Changing spot-to-plage area ratios on stars of different activity (Radick, Lockwood, & Baliunas 1989) could further effect the relative balance of $A_{\rm S}$ and $A_{\rm C}$ contributions to $A_{\rm tot}$. Our predicted $A_{\rm S}$ values will be overestimates if fluxtube emergence latitudes are restricted on rapid rotators. Differences in exactly how $v_{\rm r}$ is measured can also affect the analysis (Fig. 1; or compare, e.g., Deming & Plymate 1994, who fit IR lines, with McMillan et al. 1993, who measure the steep sides of lines in the violet).

Finally, as $A_{\rm C,max}$ and $A'_{\rm max}$ are based on extrema, they will be affected by large random noise excursions, and together with $\sigma'_{v_{\rm r}}$ will also include any intrinsic measurement noise ($\sigma \approx 13$ m s^{-1}; Walker et al. 1995). Intrinsic noise will particularly affect low amplitude $A_{\rm C,max}$, $A'_{\rm max}$, and $\sigma'_{v_{\rm r}}$ values. The number of $v_{\rm r}$ measurements for a given star is <68 in the all cases we studied, however, implying it is statistically unlikely to see excursions of $> 2\sigma$ in $A'_{\rm max}$. Thus, we expect $A'_{\rm max} \sim 2\ \sigma'_{v_{\rm r}}$, and so the good overall agreement between $A'_{\rm max}$ and $2\ \sigma'_{v_{\rm r}}$ (Fig. 4) implies that the $A'_{\rm max}$ values may not be seriously affected by any remaining large noise spikes.

4. Summary and Future Directions

Despite these uncertainties, the trends of observed maximum v_r amplitudes and dispersions, $A'_{\rm max}$ and σ'_{v_r}, which decrease with $B-V$, and increase with $v \sin i$ and activity (Fig. 4), are qualitatively similar with trends expected due to rotation and evolution of starspots (Fig. 2) and convective inhomogeneities (Fig. 3). In the few cases where we can estimate values of both A_S and A_C, there is also good quantitative agreement between their quadratic sum, $A_{\rm tot}$ and the observed $A'_{\rm max}$ value (Fig. 5). Taken together, these results support the idea that cool stars can show significant radial velocity variations due to stellar surface activity. Detection of planets is thus likely to be more difficult for certain ranges of $P_{\rm orb}$ (near those corresponding to stellar activity variations) around stars somewhat more active than the Sun, unless the star is cool (reducing A_C) and/or is inclined significantly to the line-of-sight (reducing both A_C and A_S due to lower $v \sin i$). However, even in inactive, slowly rotating stars, bisector variations will make it somewhat difficult to detect a planet with the orbit and mass of Jupiter since the amplitudes of both are roughly equal (Fig. 3). For more active stars (e.g., β Comae, ξ Boo A), planets similar to those around 51 Peg and 47 UMa would be difficult to discern against A_C for certain ranges of $P_{\rm orb}$. For $v \sin i \gtrsim 5$ km s^{-1}, spot coverage in G dwarfs increases to make $A_S \geq 20$ m s^{-1} (Fig. 2), further confusing planet searches. Thus, *there is likely a decided bias in ease of planet detection towards stars which are inactive, have low $v \sin i$, and are cooler than mid-G.* Only larger planetary velocity signals at periods well separated from magnetic timescales will detectable on active, high-$v \sin i$ stars.

Clearly, further long-term measurements of ΔV, $v_{\rm span}$, v_r, and activity are needed to confirm and extend our results. In particular, a high-precision, *simultaneous* study of $v_{\rm span}$ and v_r (the latter perhaps derived from telluric lines), would be useful to determine the true relationship between Δv_r and $v_{\rm span}$. With more data, a detailed power spectrum analysis of the $v_{\rm span}$, photometric, and v_r variations could be used to determine the velocity contributions of stellar inhomogeneities on a wide range of timescales. Towards this end, a forthcoming analysis of $v_{\rm span}$ from a long timeseries ($\sim$ 10 years) of spectra from NSO McMath–Pierce stellar spectrograph (resolution $R \geq 10^5$) should yield useful data. More realistic models of inhomogeneous stellar

surfaces are also needed, extending the work of Gray & Toner (1988) and Toner & LaBonte (1990) in the direction of Dravins & Nordlund (1990b), and studying the combined $v_{\rm r}$ effects of spots and convection.

Several techniques can be used to aid planet detection in the face of activity-related $v_{\rm r}$ variations. The simplest method is to avoid stars with large $A_{\rm C}$ (F stars and higher $v \sin i$ G stars) or large $A_{\rm S}$ (stars with significant ΔV). Roughly solar age and older G stars, and K stars with low ΔV are thus optimal. More active stars can still be studied successfully, but $v_{\rm r}$ "noise" due to activity will be higher, and proposed planets with $P_{\rm orb}$ near $P_{\rm rot}$, $P_{\rm cyc}$, or timescales of AR growth/decay will be suspect unless their reflex motion is $\gg A_{\rm tot}$. Certain methods of $v_{\rm r}$ measurement may be less affected by spots or non-uniform convection (see Dravins 1985; McMillan et al. 1994). Simultaneous multiband photometry would aid future planet searches, as luminosity and color changes correlated with $\Delta v_{\rm r}$ could be used to distinguish spots from planetary signatures (e.g., Giampapa, Craine, & Hott 1995). In cases where the AR/spot geometries are simple, the shape of $\Delta v_{\rm r}(\phi)$ may also be a useful discriminant (Fig. 1).

We are grateful for helpful discussions with Geoff Marcy, David Gray, Sallie Baliunas, Willie Soon, and Andrea Prestwich. We also thank the referee for insightful comments and suggestions which led to significant improvement of the paper. This research includes observations made at Mount Wilson Observatory, operated by the Mount Wilson Institute under an agreement with the Carnegie Institution of Washington. We are indebted to past and present members of the HK Project, without whom the long-term S measurements would not exist. SHS was supported by NSF grant AST-9528563 and NASA grant GO-5870.01-94A from STScI, which is operated by AURA, Inc., under NASA contract NAS5-26555.

Table 1. Stellar Data and Predicted Velocity Variations Due to Starspots

Name/ HD #	Spectral Type	$B-V$	$\log R'_{\rm HK}$	$v \sin i$ [km s^{-1}]	ΔV [mag]	$A_{\rm S}$ [m s^{-1}]	Refs.*
τ Boo[a]	F7V	0.48	–4.736	17	0.0011[b]	< 1	3/8
114762[a]	F9V	0.54	–4.956	1.9	0.0011[b]	< 1	1/1
β Com	G0V	0.57	–4.745	4.0	0.011	11	2,3/4
χ^1 Ori	G0V	0.58	–4.419	9.4	0.030	84	3/4
HN Peg	G0V	0.59	–4.414	10.2	0.040	$\sim$125[c]	3/4
47 UMa[a]	G1V	0.61	–5.047	1.9	0.0002[b]	< 1	1/1
π^1 UMa	G1.5V	0.62	–4.378	9.0	0.034	92	2/4
β Hyi	G2IV	0.62	–4.996[d]	$\lesssim 1.1$	< 0.006[e]	$\lesssim 1$	5/4
Sun	G2V	0.66	–4.896	2.0	0.0015	<1	4
VB 64	G2V	0.66	–4.466	5.0	0.021	26	3/4
α Cen A	G2V	0.71	–5.002[d]	2.7	< 0.005[e]	< 3	6/4
9 (BE) Cet	G3V	0.65	–4.435	6.7	0.028	50	6/4
70 Vir[a]	G4V	0.71	–5.124	0.9	0.0002[b]	< 1	1/1
15 Sge	G5V	0.61	–4.800	$\lesssim 3.7$	0.008	$\lesssim 7$	5/4
51 Peg[a]	G5V	0.67	–5.066	2.4	0.0002[b]	< 1	7/1
κ^1 Cet	G5V	0.68	–4.430	4.5	0.020	22	6/4
61 Vir	G6V	0.71	–4.999	2.0	< 0.0025[e]	< 1	2/8
τ Cet	G8V	0.72	–4.957	0.9	< 0.0025[e]	$\lesssim 1$	2/8
ξ Boo A	G8V	0.76	–4.363	2.7	0.026	15	2/9
152391	G8V	0.76	–4.446	3.7	0.02	17	6/10
ρ^1 Cnc[a]	G8V	0.86	–4.950	$\lesssim 1.1$	0.0002[b]	$\lesssim 1$	5/8

*References ($v \sin i / \Delta V$): [1] Henry et al. (1997); [2] Gray (1984); [3] Soderblom (1983); [4] Dorren & Guinan (1994a); [5] estimated from $P_{\rm rot}$; [6] Saar & Osten (1997); [7] François et al. (1996); [8] Baliunas et al. (1997); [9] Gray et al. (1996b); [10] Dorren & Guinan (1982)

[a] Possible planetary companion detected

[b] Variability not detected; the value listed is average seasonal σ.

[c] $v \sin i$ outside range of models; value approximate

[d] Henry et al. (1996)

[e] Variability not detected; the value listed is the upper limit to the amplitude.

Table 2. Stellar Data and Velocity Variations: Predicted (from Line Bisectors) and Observed (from Walker et al. 1995)

Name/ HD #	Spec. Type	$B-V$	$\log R'_{\rm HK}$	$v \sin i$ [km s^{-1}]	$A_{\rm C,rot}$ [m s^{-1}]	$A_{\rm C,max}$ [m s^{-1}]	$A'_{\rm max}$ (obs.) [m s^{-1}]	σ'_{v_r} (obs.) [m s^{-1}]	Refs.*
36 UMa	F8V	0.52	−4.884	$\leq$3.0	···	···	46	18	1
β Vir	F8V	0.55	−4.940	3.2	···	···	52	22	2
β Com	G0V	0.57	−4.745	4.0	···	55	44	17	2,3/4
χ^1 Ori	G0V	0.58	−4.419	9.4	100	100	50[a]	24[a]	3/5
ι Per	G0V	0.59	−5.091	3.5	···	···	34	17	3
Sun	G2V	0.66	−4.896	2.0	<10[b]	7[b]	···	···	6
51 Peg	G5V	0.67	−5.066	2.4	<10	<10	···	···	7/8
κ^1 Cet	G5V	0.68	−4.430	4.5	···	···	53	20	9
61 Vir	G6V	0.71	−4.998	2.0	···	···	32	17	2
τ Cet	G8V	0.72	−4.955	0.9	<10	15	38	12	2
ξ Boo A	G8V	0.76	−4.363	2.7	32	47	65[a]	22[a]	2/10,11
σ Dra	K0V	0.79	−4.829	1.5	<10	17	29	13	2/12
40 Eri A	K1V	0.82	−4.882	1.4	···	···	30	16	9
36 Oph A	K1V	0.85	−4.567	0.8	···	···	36[a]	16[a]	9
36 Oph B	K1V	0.86	−4.559	1.4	···	···	53[a]	22[a]	9
ϵ Eri	K2V	0.88	−4.458	1.7	<12	21	39	15	9/13
219134	K3V	1.01	−4.974	$\leq$0.7	···	···	31	14	14
61 Cyg A	K5V	1.18	−4.761	$\leq$1.0	···	···	51[a]	21[a]	14
61 Cyg B	K7V	1.37	−4.897	$\leq$0.9	···	···	34[a]	15[a]	14

*References ($v \sin i$/bisector): [1]SIMBAD database; [2]Gray (1984); [3]Soderblom (1983); [4]Gray et al. (1996a); [5]Bruning & Saar (1990); [6]Livingston (1991); [7]François et al. (1996); [8]Hatzes et al. (1997); [9]Saar & Osten (1997); [10]Gray et al. (1996b); [11]Toner & Gray (1988); [12]Gray et al. (1992); [13]Gray & Baliunas (1995); [14]estimated from $P_{\rm rot}$

[a]Value uncertain due to significant correction for binary motion.

[b]May not be directly comparable to the stellar data due to much higher spectral resolution (10^6).

REFERENCES

Allen, C.W. 1976, Astrophysical Quantities, (London: Athlone)

Baliunas, S.L., Donahue, R.A., Soon, W.H., et al. 1995, ApJ, 438, 269

Baliunas, S.L., Henry, G.W., Donahue, R.A., Fekel, F.C., & Soon, W.H. 1997, ApJ, 474, L119

Brandt, P.N., & Solanki, S.K. 1990, A&A, 231, 221

Bruning, D.H. 1984, ApJ, 281, 830

Bruning, D.H., & Saar, S.H. 1990, in ASP Conf. Ser. 9, Cool Stars, Stellar Systems and the Sun, ed. G. Wallerstein (San Francisco: ASP), 165

Butler, R.P., Marcy, G.W., Williams, E., Hauser, H., & Shirts, P. 1997, ApJ, 474, L115

Butler, R.P., Marcy, G.W., Williams, E., McCarthy, C., Dosanjh, P., & Vogt, S.S. 1996, PASP, 108, 500

Butler, R.P., & Marcy, G.W. 1996, ApJ, 464, L153

Bünte, M., & Saar, S.H. 1993, A&A, 271, 167

Campbell, B., Walker, G.A.H., & Yang, S. 1988, ApJ, 331, 902

DeLuca, E.E., Fan, Y., Saar, S.H. 1997, ApJ, in press (May 20).

Deming, D., Espenak, F., Jennings, D.E., Brault, J.W., & Wagner, J. 1987, ApJ, 316, 771

Deming, D., & Plymate, C. 1994, ApJ, 426, 382

Dempsey, R.C., Bopp, B.W., Strassmeier, K.G., Granados, A.F., Henry, G.W., & Hall, D.S. 1992, ApJ, 392, 187

Dobson, A.K., Donahue, R.A., Radick, R.R., & Kadlec, K.L. 1990, in ASP Conf. Ser. 9, Cool Stars, Stellar Systems and the Sun, ed. G. Wallerstein (San Francisco: ASP), 132

Donahue, R.A. 1993, Ph.D. thesis, New Mexico State Univ.

Donahue, R.A., & Baliunas, S.L. 1992, Sol. Phys., 141, 181

Donahue, R.A., Saar, S.H., & Baliunas, S.L. 1996, ApJ, 466, 384

Donahue, R.A., Dobson, A.K., & Baliunas, S.L. 1997, Sol. Phys., in press

Dorren, J.D., & Guinan, E.F. 1982, AJ, 87, 1546

Dorren, J.D., & Guinan, E.F. 1994a, in The Sun as a Variable Star: Solar and Stellar Irradiance Variations, eds. J.M. Pap, C Fröhlich, H.S. Hudson, S.K. Solanki (Cambridge: Cambridge Univ. Press), 206

Dorren, J.D., & Guinan, E.F. 1994b, ApJ, 428, 805

Dravins, D. 1985, in IAU Colloq. 88, Stellar Radial Velocities, eds. A.G.D. Philip & D.W. Latham (Schenectady: L. Davis Press), p. 5

Dravins, D. & Nordlund, Å. 1990a, A&A, 228, 184

Dravins, D. & Nordlund, Å. 1990b, A&A, 228, 218

Eddy, J.A. 1977, in The Solar Output and Its Variation, ed. O.R. White (Boulder: Colo. Univ. Press), 51

François, P., Spite, M., Gillet, D., Gonzalez, J.-F., & Spite, F. 1996, A&A, 310, L13

Giampapa, M.S., Craine, E.R., Hott, D.A. 1995, Icarus, 118, 199

Gray D.F. 1982, ApJ, 255, 200

Gray D.F. 1984, ApJ, 281, 719

Gray D.F. 1986, PASP, 98, 319

Gray, D.F. 1988, Lectures on Spectral Line Analysis: F, G, and K Stars, (Arva, Ontario: The Publisher)

Gray, D.F., & Baliunas, S.L. 1994, ApJ, 427, 1042

Gray, D.F., & Baliunas, S.L. 1995, ApJ, 441, 436

Gray, D.F., Baliunas, S.L., Lockwood, G.W., & Skiff, B.A. 1992, ApJ, 400, 681

Gray, D.F., Baliunas, S.L., Lockwood, G.W., & Skiff, B.A. 1996a, ApJ, 456, 365

Gray, D.F., Baliunas, S.L., Lockwood, G.W., & Skiff, B.A. 1996b, ApJ, 465, 945

Güdel, M., Schmitt, J.H.M.M., Benz, A.O., & Elias II, N.M. 1995, A&A, 301, 201

Hatzes, A.P. 1996, PASP, 108, 839

Hatzes, A.P., Cochran, W.D., & Johns-Krull, C.M. 1997, ApJ, in press.

Henry, G.W., Baliunas, S.L., Donahue, R.A., Soon, W., & Saar, S.H. 1997, ApJ, 474, 503

Henry, T.J, Soderblom, D.R., Donahue, R.A., & Baliunas, S.L. 1996, AJ, 111, 439

Irwin, A.W., Yang, S., Walker, G.A.H. 1992, PASP, 104, 101

Livingston, W. 1982, Nature, 297, 208

Livingston, W. 1991, in The Sun and Cool Stars: Activity, Magnetism, Dynamos, eds. I. Tuominen, D. Moss, & G. Rüdiger (Dordrecht: Springer), 246

Marcy, G.W., & Butler, R.P. 1996, ApJ, 464, L147

Mayor, M., & Queloz, D. 1995, Nature, 378, 355

McMillan, R.S., Moore, T.L., Perry, M.L., & Smith, P.H. 1993, ApJ, 403, 801

McMillan, R.S., Moore, T.L., Perry, M.L., & Smith, P.H. 1994, Ap&SS, 212, 271

Nordlund, Å, & Dravins, D. 1990, A&A, 228, 135

Noyes, R.W., Hartmann, L., Baliunas, S.L., Duncan, D.K., & Vaughan, A.H. 1984, ApJ, 279, 763

O'Dell, M.A., Panagi, P., Hendry, M.A., & Collier-Cameron, A. 1995, A&A, 294, 715

O'Neal, D., Saar, S.H., & Neff, J.E. 1996, ApJ, 463, 766

Radick, R.R., Lockwood, G.W., & Baliunas, S.L. 1989, Science, 247, 39

Ruciński, S.M., & VandenBerg, D.A. 1986, PASP, 98, 669

Saar, S.H., & Bruning, D.H. 1990, in ASP Conf. Ser. 9, Cool Stars, Stellar Systems and the Sun, ed. G. Wallerstein (San Francisco: ASP), 168

Saar, S.H., & Osten, R.A. 1997, MNRAS, in press (Feb. 1)

Schüssler, M., & Solanki, S.K. 1992, 263, L13

Skumanich, A. 1972, ApJ, 171, 565

Soderblom, D.R. 1983, ApJS, 53, 1

Smith, M.A., Huang, Y.-R., & Livingston, W. 1987, PASP, 98, 297

Strassmeier, K.G. 1996, in Stellar Surface Structure, eds. K.G. Strassmeier and J.L. Linsky, (Dordrecht: Kluwer), p. 289

Strassmeier, K.G., Hall, D.S., Fekel, F.C., & Scheck, M. 1993, A&AS, 100, 173

Toner, C.G. & Gray D.F. 1988, ApJ, 334, 1008

Toner, C.G. & LaBonte, B.J. 1990, in ASP Conf. Ser. 9, Cool Stars, Stellar Systems and the Sun, ed. G. Wallerstein (San Francisco: ASP), 161

Vogt, S.S., Penrod, G.D., Hatzes, A.H. 1987, ApJ, 321, 496

Walker, G.A.H., Walker, A.R., Irwin, A.W., Larson, A.M., Yang, S.L.S., & Richardson, D.C. 1995, Icarus, 116, 359

This manuscript was prepared with the AAS LaTeX macros v4.0.

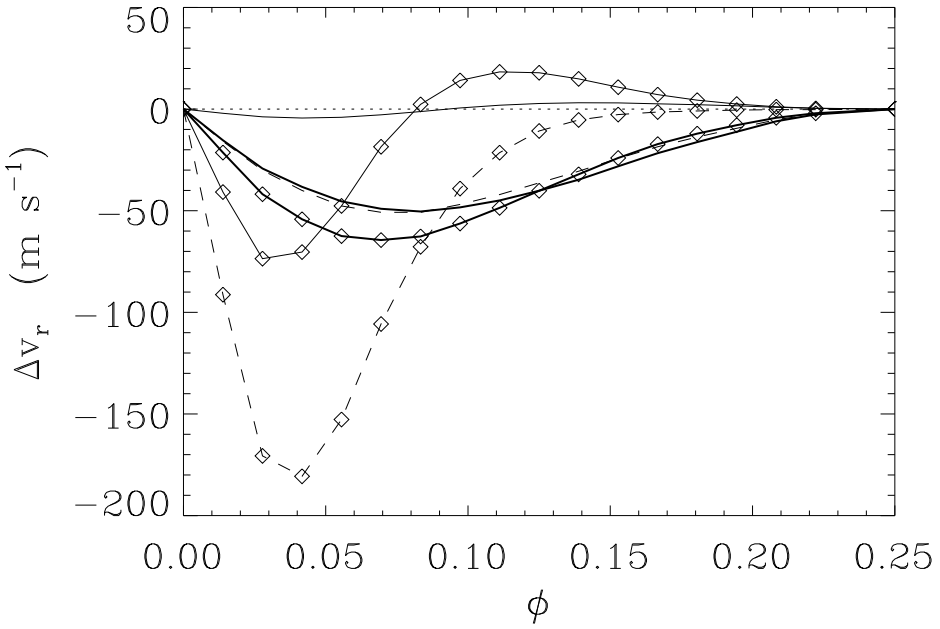

Fig. 1.— Δv_r versus rotational phase ϕ for a spotted G star model with $f_S = 1\%$ and $v \sin i = 3$ km s^{-1} (simple curves) and 9 km s^{-1} (curves with diamonds overplotted) using several measures of v_r: Gaussian fit to the line (thick solid), line center interpolation (dashed), and $v_{span}/2$ (thin solid). For ease of comparison, Δv_r for the $v \sin i = 3$ km s^{-1} models has been multiplied by 3 (following eqn. 1), and $\Delta v_r = 0$ is indicated (dotted line). Note the sharply stronger dependence of Δv_r on $v \sin i$ for the line center and v_{span} methods, and the differences in $\Delta v_r(\phi)$.

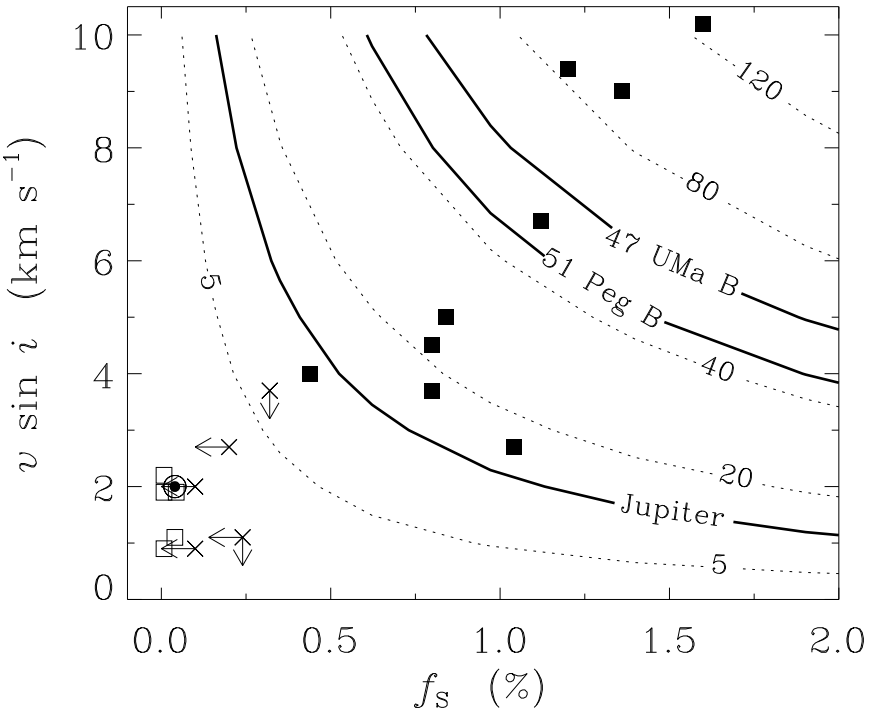

Fig. 2.— Contours (labeled in m s^{-1}) of the estimated radial velocity perturbation amplitude, A_S, due to the rotation of equatorial starspots with $T_S = 0$ on G stars as a function of spot area f_S and $v \sin i$. Data for the Sun ($\odot$) and a sample of G dwarfs are also shown (using $f_S \approx 0.4\Delta V$): stars with measured photometric amplitude (filled squares), stars with upper limits to ΔV or $v \sin i$ (crosses), and stars with newly detected planetary companions and upper limits to ΔV (open squares). The A_S contours corresponding to the amplitude of the solar/stellar reflex motions due to Jupiter, and the companions to 51 Peg and 47 UMa are also shown for comparison (heavy solid lines). For stars more active than the Sun, especially those younger than $\sim$ 1 Gyr, A_S increases dramatically.

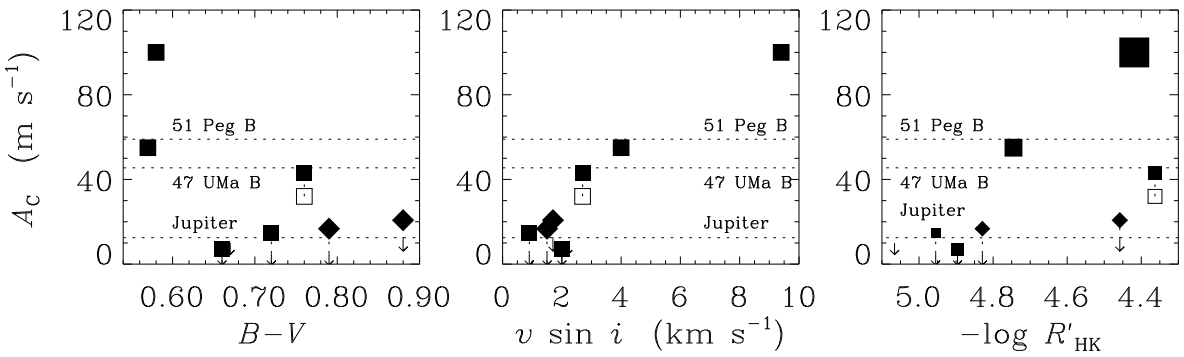

Fig. 3.— Estimated v_r perturbation amplitudes, A_C, due to non-uniform convection as estimated from variable line bisectors (G stars: □; K stars: ◇), plotted versus $B-V$ color (left), $v \sin i$ (center), and normalized Ca II HK flux, $\log R'_{HK}$ (right, where symbol size scales with $v \sin i$). Both the rotational modulation (open symbol or upper limit) and the maximum observed A_C (filled symbol) are shown, where available, connected with a dotted line. Also shown are the v_r amplitudes corresponding to the reflex amplitudes caused by Jupiter and two of the newly discovered planets (horizontal dashed lines).

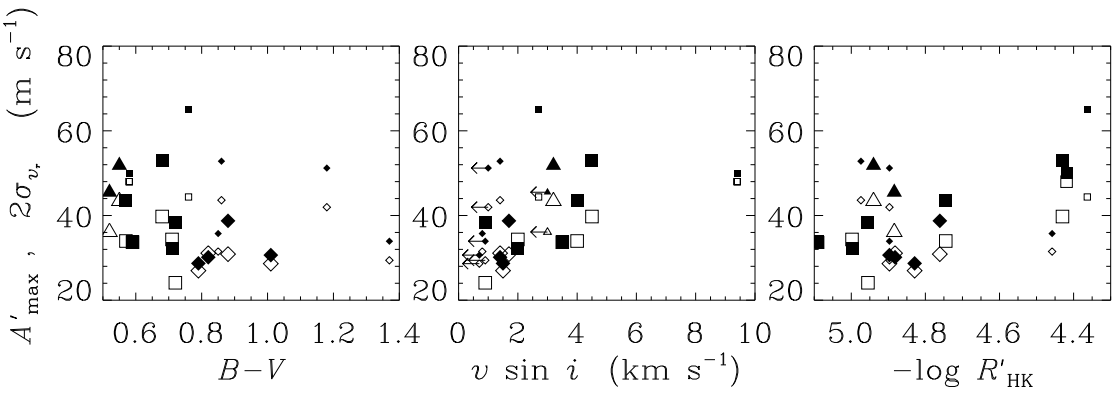

Fig. 4.— Observed velocity range amplitude $A'_{\rm max}$and rms σ'_{v_r} (F dwarfs: △, G dwarfs: □, K dwarfs: ◇; filled symbols are $A'_{\rm max}$), computed from data in Walker et al. (1995), are plotted against $B-V$ (left), $v \sin i$ (center), and normalized Ca II HK flux, $\log R'_{\rm HK}$ (right). Motions due to binary companions have been removed (these points plotted at half size due to their reduced accuracy), and 2 σ'_{v_r} is shown for ease of comparison. $A'_{\rm max}$ and σ'_{v_r} appear to increase with $v \sin i$, $T_{\rm eff}$, and with chromospheric activity.

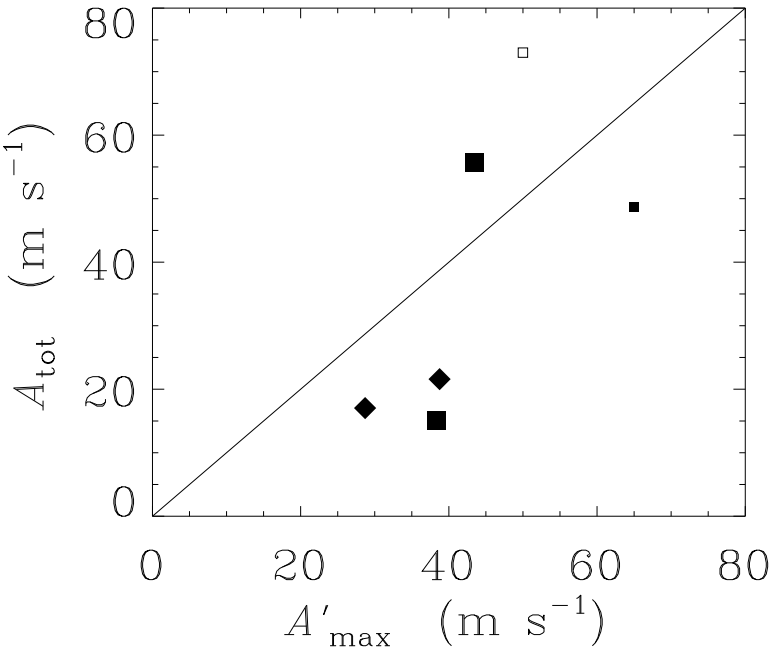

Fig. 5.— Observed maximum $v_{\rm r}$ amplitude $A'_{\rm max}$ (computed from Walker et al. 1995 data) versus estimated total $v_{\rm r}$ amplitude $A_{\rm tot}$, based on the combined effects of spot and bisector variations ($A_{\rm tot} = \sqrt{(A_{\rm S})^2 + (A_{\rm C,max})^2}$; G dwarfs: □, K dwarfs: ◇, symbols for binaries are plotted at half size). The relation $A'_{\rm max}$= $A_{\rm tot}$ is shown for comparison; rms about this line is $\sigma \approx 14$ m s^{-1}, consistent with the mean internal errors of the Walker et al. data. A "corrected" $A_{\rm tot}$ value (see text) for the binary χ^1 Ori is plotted as an open symbol, but not included in the rms calculation.